Journal of Engineering Mathematics **38:** 265–278, 2000.

Waves of high frequency in suspensions near the critical point of the particulate pressure-density dependence

P. VAINSHTEIN, M. SHAPIRO and C. GUTFINGER
Faculty of Mechanical Engineering, Technion – Israel Institute of Technology, Haifa 32000 Israel

Received 2 February 1999; Accepted in revised form 22 december 1999

Abstract. The paper considers theoretically the propagation of weakly nonlinear high-frequency waves in homogeneous gas-solid suspensions. The governing equations include the equation of particle conservation and the equation of mean motion of the particles. These equations are supplemented by a barotropic dependence of the particulate pressure on the particle volume fraction which has a point of maximum (critical point) separating the regions of increase and decrease of the particulate pressure. Under condition that the particulate gas viscosity is negligible, the conservation laws represent a system of mixed hyperbolic-elliptic type. It is shown that a uniformly fluidized bed operated at the critical concentration is unstable with respect to high-frequency sinusoidal oscillations.

Key words: waves, high frequency, suspensions, particulate pressure, critical point, equations of mixed type

1. Introduction

Wave propagation in suspensions of particles in fluids has been a subject of extensive studies for a long time. Various investigations have dealt with long waves of arbitrary amplitude and small-amplitude waves of arbitrary wavelength.

Long-wave propagation in suspensions during sedimentation was studied first theoretically by Kynch [1]. He assumed that the mean vertical sedimentation velocity of the particles is equal to the mean velocity of a uniform suspension where gravity, which drives the motion, is balanced by the mean drag force exerted by the fluid on the particles. As a result, wave motion is governed by one nonlinear equation for the particle-volume fraction α_s, where the wave speed is a function of α_s. This is an example of kinematic waves which were studied thoroughly by Lighthill and Whitham [2]. Comprehensive reviews on this subject were given by Ganser and Drew [3], Kluwick [4] and Harris and Crighton [5].

Investigations of the behavior of small-amplitude waves deal mainly with the stability of particle sedimentation. For higher-frequency disturbances, the effect of particle inertia causes some delay in the adjustment of the mean particle velocity to the rapidly changing local concentration. In the limit of high-frequency disturbances, the inertial forces prevail over gravity and drag force. Such waves are called dynamic waves. If the basic flow is stable, the decay rate of the disturbances at large times is governed by kinematic waves [2]. On the other hand, if the basic flow is unstable, the growth of disturbances is determined by dynamic waves (Kluwick [6]).

Propagation of a small disturbance within a uniform fluidized bed was first calculated by Jackson [7] using equations of continuity and momentum of the particulate phase. The momentum equation accounted for gravity, drag force and inertial forces. The analysis revealed that the state of uniform fluidization is always unstable due to particle inertia.

Carg and Pritchett [8] showed that it is possible to predict stability limits if particulate pressure due to particle-particle interactions is taken into account. Batchelor [9] first introduced a specific barotropic equation in the context of the stability analysis relating particulate pressure to its volume fraction. The equation has a point of maximum (critical point) separating the regions in which the particulate pressure increases and decreases as the volume fraction increases. Such equations have recently been experimentally verified by Zenit et al. [10]. Paper [9] considered the limiting case of disturbances of very high frequency when gravity, drag force, as well as the effect of particulate gas viscosity are negligible altogether. For that case the governing equations, including those of particulate continuity and momentum equations, comprise a system of mixed hyperbolic-elliptic type. These equations are elliptic in the region where the pressure decreases with increasing density. In this region any perturbation continues to grow under ensuing pressure drop leading to instability [9]. This paper contains also a comprehensive survey of works on the stability problem of uniform fluidized beds.

In the hyperbolic region, a uniform fluidized bed may be either stable or unstable, depending on the relevant criterion of stability [9]. Fanucci et al. [11] studied numerically nonlinear wave propagation in the hyperbolic region using the method of characteristics. They showed that initially sinusoidal wavetrains may evolve into a shock fronts due to nonlinear effects. This problem was treated analytically in [6]. In particular, the author considered small-amplitude high-frequency periodic waves when the particulate inertia, as well as gravity and drag force are taken into account. It was shown that if the basic flow is unstable, periodic disturbances approach the form of a constant amplitude saw-tooth non-decaying in time.

Batchelor's stability analysis of uniformly fluidized beds considers regions far from the critical point where particle velocity and volume fraction are of the same orders of magnitude. In the vicinity of the critical point this analysis is invalid (Lammers and Biesheuvel [14]). A specific goal of the present work is to investigate nonlinear one-dimensional wave propagation in a homogeneous unconfined fluidized bed near the point of maximum of the dependence $p_s = p_s(\alpha_s)$ where both the hyperbolic and elliptic regions are important. Near this point particle velocity and volume fraction are of different orders of magnitude and the perturbation procedure employed in [9] is no longer applicable. This study is aimed at stability analysis of a uniformly fluidized bed at a critical concentration and evolution of initially sinusoidal wavetrains towards some stationary regime which occurs as a result of the instability.

We consider the limiting case of disturbances of very high frequency when gravity and drag forces are negligible to analyze the evolution and the ultimate form of these wavetrains. Such analysis is important, since in practice fluidized-bed operation near critical concentration is attractive for practical applications (see review in [13]).

The paper is organized as follows. A set of equations describing the mean flow of gas-solid suspensions and a statement of the problem are presented in Section 2. Equations for small-amplitude high-frequency waves are derived in Section 3. Analytical solutions of these equations describing steady-state, self-similar and simple waves are considered in Section 4, together with numerical simulations of small-amplitude periodic wave motions in a uniformly fluidized-bed resulting in its instability. The discussion and conclusion sections summarize the results obtained.

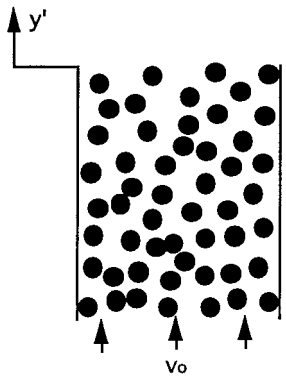

Figure 1. Schematic of a fluidized bed domain with coordinate system.

2. Problem formulation and governing equations

Consider a bed of identical solid particles fluidized in a vertical pipe of constant cross-section where variations of the field quantities in directions perpendicular to the pipe axis are sufficiently small to be negligible. Thus, a one-dimensional treatment is appropriate. Furthermore, it is assumed that both gas and solid phases are incompressible. The flow can be adequately described by governing equations for mixtures proposed in the previous studies (see [9, 13]). It follows from these equations that the gas and particle conservation equations have an integral

$$(1-\alpha_s)v'_g + \alpha_s v'_s = v_o = \text{const}, \tag{2.1}$$

where v'_g, v'_s are the gas and particle velocities, respectively, α_s is the particle volume fraction and v_o is the average velocity of the suspension. Equation (2.1) enables one to express the gas velocity in terms of the particle volume fraction and particle velocity allowing the particle mass and momentum equations to be treated independently. These equations have the following form

$$\frac{\partial \alpha_s}{\partial t'} + \frac{\partial \alpha_s v'_s}{\partial y'} = 0, \tag{2.2}$$

$$\rho_s^o \alpha_s \left(\frac{\partial v'_s}{\partial t'} + v'_s \frac{\partial v'_s}{\partial y'} \right) = -\frac{\partial p'_s}{\partial y'} + n f_\mu - \rho_s^o \alpha_s g + \frac{\partial}{\partial y'} \left(\alpha_s \mu_s \frac{\partial v'_s}{\partial y'} \right), \tag{2.3}$$

where y', t' denote the spatial coordinate as measured along the pipe axis (see Figure 1) and time; ρ_s^o is the particle density, p'_s is the particulate pressure, n is the particle number density, f_μ is the drag force acting on the particle, g is the gravitational acceleration and μ_s is the particulate gas viscosity coefficient. For small particles, shear stresses are, generally, much smaller than those associated with the particulate pressure (see [14]). We will, therefore, neglect the terms related to particulate gas viscosity.

Note that one can also employ the one-dimensional fluid momentum equation (see *e.g.*, [13]) to analyze the gas motion on the fluidized bed. We may treat this equation separately, using results obtained from the analysis of Equations (2.2), (2.3), which provide therefore a sufficiently general model of the fluidized bed.

Equations (2.2), (2.3) are to be closed by a relationship between the particulate pressure and volume fraction. This particulate pressure is associated with the particle velocity fluctuations

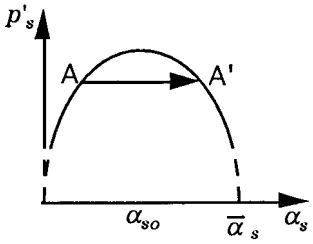

Figure 2. Dependence of the particulate pressure on the particle volume fraction.

and interparticle collisions. Generally, known approximate kinetic models of dense gases may be used to determine the equation of state of the particulate suspension and the expression for particle kinetic energy [15, pp. 87–104]. When the rates of production and dissipation of the particulate kinetic energy are equal, the particulate pressure and the particle volume fraction are connected by a barotropic relationship [13]. A particular form of such a phenomenological relationship, proposed in [9], is used in this paper

$$p'_s = \rho_s^o \alpha_s U_s^2 \frac{\alpha_s}{\overline{\alpha}_s}\left(1 - \frac{\alpha_s}{\overline{\alpha}_s}\right), \tag{2.4}$$

where $\overline{\alpha}_s$ is the particle volume fraction of the packed bed. This relationship is shown qualitatively in Figure 2. U_s is the mean particle velocity in a homogeneous fluidized bed given by the experimental correlation [16]:

$$U_s = v_o - u_t(1 - \alpha_s)^\gamma, \tag{2.5}$$

where γ is an empirically determined constant, dependent *inter alia* on the particle Reynolds number and u_t is the terminal velocity of a single particle in a quiescent gas. Note, that if $v_o = 0$, U_s in (2.5) represents the mean velocity of freely precipitating particles. For large particle Reynolds number u_t may be given by the empirical relation

$$u_t = \left(\frac{16}{3}\frac{\rho_s^o}{\rho_g^o} rg\right)^{1/2}, \tag{2.6}$$

where ρ_g^o is the gas density and r is the particle radius. Equation (2.4) describes qualitatively the dependence of the particulate pressure on the volume fraction, reflecting the most important property of the particulate pressure, of vanishing at $\alpha_s \to 0$ and $\alpha_s \to \overline{\alpha}_s$. The particulate pressure, p'_s, has a maximum at $\alpha_s = \alpha_{so}$ where the speed of sound waves in the particulate gas vanishes, namely $\alpha_{so}/\overline{\alpha}_s = \frac{2}{3}$.

The model employed here is valid only for volume fractions insignificantly different from α_{so}, i.e., for fluidization regime differing from the packed-bed state and from the situation where α_s is close to zero. Accordingly, the particulate pressure (2.4) does not reduce to the hydrostatic pressure for zero fluidization velocity. Therefore, the behavior of the function $p'_s(\alpha_s)$ near the points $\alpha_s = \overline{\alpha}_s$ and also $\alpha_s = 0$ and are unimportant for the present study. Corresponding regions are shown in Figure 2 by dashed lines. Further discussion on this matter may found in [13] and papers cited therein.

For further analysis we define the following dimensionless variables and parameters

$$Y = \frac{y'g}{U_0^2}, \quad T = \frac{t'g}{U_0}, \quad v = \frac{v'_s g}{U_0}, \tag{2.7}$$

where U_0 is a velocity to be specified below. We also define $\alpha = \alpha_s/\overline{\alpha}_s$, where $\alpha = \alpha_0 = 2/3$ corresponds to the critical point. Using (2.1), (2.4), (2.5), we may represent Equations (2.2) and (2.3) in the forms [9]

$$\frac{\partial \alpha}{\partial T} + \frac{\partial \alpha v}{\partial Y} = 0, \tag{2.8}$$

$$\frac{\partial v}{\partial T} + v\frac{\partial v}{\partial Y} + \frac{C(\alpha)}{\alpha}\frac{\partial \alpha}{\partial Y} = \left[\frac{U_0^2(v - v_o/U_0)^2}{u_t^2(1 - \alpha\overline{\alpha}_s)^{2\gamma}} - 1\right], \tag{2.9}$$

where $C(\alpha)$ is the square of the dimensionless speed of sound associated with the particle flow:

$$C(\alpha) = \frac{1}{\rho_s^o U_0^2}\frac{\mathrm{d}p_s'}{\mathrm{d}\alpha_s}. \tag{2.10}$$

System (2.8), (2.9) is identically satisfied by the solution

$$\alpha = \alpha_a = \text{const}, \quad v = v_a = \frac{U_{sa}}{U_0}, \tag{2.11}$$

where U_{sa} is given by (2.5). At these values the right-hand side of (2.9) vanishes. Therefore, Equation (2.11) constitutes a steady-state and uniform solution of (2.8), (2.9), corresponding to that of a homogeneous fluidized bed. Generally, $\alpha_a \neq \alpha_0$; however, in some cases $\alpha_a = \alpha_0$ (see below). In all cases $|\alpha_a - \alpha_0| \ll 1$.

We study the behavior of small perturbations of the homogeneous solution (2.11) resulting from an initial condition $\alpha(0, Y)$ slightly different from α_a so that

$$0 < \varepsilon = \max|\alpha(0, Y) - \alpha_0| \ll 1. \tag{2.12}$$

The problem of evolution of a small perturbation in a homogeneous suspension is treated in the limit when the dimensionless characteristic time of the disturbance, denoted as Ω^{-1} is very small, i.e. $\Omega \to \infty$. The limiting procedure is ordered such that

$$\Omega^{-1} \ll \varepsilon. \tag{2.13}$$

In this case Equations (2.8), (2.9) may be significantly simplified before the perturbation procedure is applied with respect to the small parameter ε developed in the next section. In order to describe the approach of Ω to infinity, we now define new variables

$$t = \Omega T, \quad y = \Omega Y, \quad \Omega \to \infty, \tag{2.14}$$

Then, Equations (2.8), (2.9) take the form

$$\frac{\partial \alpha}{\partial t} + \frac{\partial \alpha v}{\partial y} = 0, \tag{2.15}$$

$$\frac{\partial v}{\partial t} + v\frac{\partial v}{\partial y} + \frac{C(\alpha)}{\alpha}\frac{\partial \alpha}{\partial y} = \frac{1}{\Omega}\left[\frac{U_0^2(v - v_o/U_0)^2}{u_t^2(1 - \alpha\overline{\alpha}_s)^{2\gamma}} - 1\right]. \tag{2.16}$$

In the limit $\Omega \to \infty$ the terms on the right-hand side in (2.16) become negligible, leading to

$$\frac{\partial v}{\partial t} + v\frac{\partial v}{\partial y} + \frac{C(\alpha)}{\alpha}\frac{\partial \alpha}{\partial y} = 0. \tag{2.17}$$

The above approximation describes a small-amplitude process occurring so fast that the effects of gravity and drag force, as expressed by the r.h.s. of (2.16), are negligible. This approximation is, therefore, valid when

$$t \ll \Omega \to \infty. \tag{2.18}$$

In particular, Equations (2.15), (2.17) will be used for the analysis of small-amplitude waves propagating in an initially uniform suspension. We shall also consider steady-state solutions of these equations in a moving frame which can be understood as asymptotic limits of wavy motions. Then, a transient time from an initial disturbance to steady-state solutions must satisfy (2.18). For large Ω unsteady flow patterns can approach their limiting steady-state form. It should be noted, however, that corresponding steady-state patterns cannot exist for a long time, because of condition (2.18). The small term neglected on the right-hand side of (2.16), associated with gravity and drag force, will disturb eventually the steady-state solutions. Thus, such steady-state solutions may be considered as intermediate asymptotics.

3. Equations for small-amplitude waves in the vicinity of the critical point

The system (2.15), (2.17) supplemented by Equations (2.4), (2.10) was analyzed for stability of the uniform state (2.11) in [9] in the linear approximation. The author assumed that disturbances of particle volume fraction and velocity are of the same order of magnitude and showed that wave velocities associated with (2.15), (2.17) are $v_a \mp \sqrt{C(\alpha_a)}$. If $\alpha_a < \alpha_0$, a small disturbance propagates with no change of form with the speed of sound in a moving frame connected with v_a. If $\alpha_a > \alpha_0$, then $C(\alpha) < 0$, implying exponential growth of a non-propagating disturbance, *i.e.*, instability. At the critical point $\alpha_a = \alpha_0$, where the speed of sound vanishes, the disturbance is frozen, that is, it moves without change of form together with the particulate gas with v_a. However, near the critical point a nonlinear analysis is necessary to study the wave motion. Here we analyze the behavior of the solution in the vicinity of the critical point, where, as we will show below, the volume fraction and the velocity disturbances are of different orders of magnitude.

Assume that in the vicinity of $\alpha_a = \alpha_0$, we may write $C(\alpha)$ in the form

$$C(\alpha) = \left(\frac{\mathrm{d}C(\alpha)}{\mathrm{d}\alpha}\right)_{\alpha=\alpha_0} (\alpha - \alpha_0) + O(\alpha - \alpha_0)^2. \tag{3.1}$$

As follows from (2.4), (2.10) $\mathrm{d}C/\mathrm{d}\alpha \mid_{\alpha=\alpha_0} \neq 0$. Note that the analysis given below is applicable to any barotropic process where the pressure-density relationship has a maximum. Without loss of generality, we choose the characteristic velocity U_0 appearing in (2.10) so that $\mathrm{d}C/\mathrm{d}\alpha \mid_{\alpha=\alpha_0} = -2\alpha_0$. The characteristic velocity U_0 can be calculated explicitly for each physical situation. As an example, consider 2·5 mm solid particles with the density ρ_s^o exceeding 10^3 times that of the gas, flowing at $v_0 = 12$ m s^{-1}. Under these conditions the terminal settling velocity given by (2.6) is 11·43 m s^{-1}, and the mean particle velocity in the flowing gas, as evaluated from (2.5) with $\gamma = 2{\cdot}5$ is $U_s = 7{\cdot}85$ m s^{-1}. This yields the characteristic velocity U_0 appearing in (2.7) equal to 9·6 m s^{-1}. With the above expression for $(\mathrm{d}C/\mathrm{d}\alpha \mid_{\alpha=\alpha_0}$ Equation (2.17) takes the form

$$\frac{\partial v}{\partial t} + v\frac{\partial v}{\partial y} + \frac{2\alpha_0(\alpha_0 - \alpha)}{\alpha}\frac{\partial \alpha}{\partial y} = 0. \tag{3.2}$$

To determine the orders of magnitude of the flow parameters in the vicinity of the critical point, we note that Equations (2.15), (2.17) have the simple wave integral relation for $\alpha < \alpha_0$

$$v = \pm \int \frac{\sqrt{C(\alpha)}}{\alpha} d\alpha. \tag{3.3}$$

We show below that, in contrast to Batchelor's analysis, Equation (3.3) yields that α and v are of different orders of magnitude. Towards this goal we substitute

$$\alpha = \alpha_0 + \varepsilon\alpha_1(y, t), \quad \alpha_1 \leq 0, \tag{3.4}$$

with ε defined in (2.12), and (3.1) in (3.3), linearize about α_0 and integrate to obtain the velocity

$$v = v_{a0} + \varepsilon^{3/2} v_1, \quad v_1 = \mp\sqrt{\frac{2}{\alpha_0}}(-\alpha_1)^{3/2} \tag{3.5}$$

where α_1 and v_1 are perturbation solutions of the first order; v_{a0} is determined by substitution of $\alpha_a = \alpha_0$ in (2.11). This result shows that in the vicinity of the maximum point the perturbation of the velocity scales as $O(\varepsilon^{3/2})$ when the perturbation of the volume fraction scale is $O(\varepsilon)$. This is in contrast with the perturbation relationships of Batchelor where $v - v_a = O(\varepsilon)$. Equation (3.5) determines the relationship between disturbances of particle velocity and particle volume fraction in the simple wave near the critical point.

In order to obtain the solution of (2.15), (3.2), we define the coordinate system attached to the uniform flow

$$t = t, \quad \varsigma = y - v_a t. \tag{3.6}$$

Then, Equations (2.15), (3.2) become

$$\frac{\partial \alpha}{\partial t} - v_a \frac{\partial \alpha}{\partial \varsigma} + \frac{\partial \alpha v}{\partial \varsigma} = 0, \tag{3.7}$$

$$\frac{\partial v}{\partial t} - v_a \frac{\partial v}{\partial \varsigma} + v\frac{\partial v}{\partial \varsigma} + \frac{2\alpha_0(\alpha_0 - \alpha)}{\alpha}\frac{\partial \alpha}{\partial \varsigma} = 0. \tag{3.8}$$

Bearing in mind (3.4), (3.5), we further assume asymptotic expressions of the form

$$\begin{aligned} \alpha &= \alpha_0 + \varepsilon\alpha_1(\varsigma, \tau) + O(\varepsilon^2), \quad \tau = \sqrt{\varepsilon}t, \\ v &= v_{a0} + \varepsilon^{3/2} v_1(\varsigma, \tau) + O(\varepsilon^2) \end{aligned} \tag{3.9}$$

to hold in the hyperbolic ($\alpha_1 < 0$) and elliptic ($\alpha_1 > 0$) regions, including the critical point. Here α_1 and v_1 are to be determined. Substitute (3.9) in (3.7), (3.8) and rearrange to obtain

$$\frac{\partial \alpha_1}{\partial \tau} + \alpha_0 \frac{\partial v_1}{\partial \varsigma} = 0, \tag{3.10}$$

$$\frac{\partial v_1}{\partial \tau} - \frac{\partial \alpha_1^2}{\partial \varsigma} = 0. \tag{3.11}$$

The initial value problems posed for the system of Equations (3.10), (3.11) are considered in the next section. Now we note that this system is nonlinear and of mixed type; hyperbolic in

the region $\alpha_1 < 0$, and elliptic in the region $\alpha > 0$. In the former region the characteristics of these equations are given by

$$\frac{d\varsigma}{d\tau} = \pm\sqrt{-2\alpha_0\alpha_1}. \tag{3.12}$$

Defining the velocity potential as

$$v_1 = \frac{\partial\phi_1}{\partial\varsigma}, \tag{3.13}$$

We can also represent Equations (3.10), (3.11) in the form

$$\frac{\partial\alpha_1}{\partial\tau} + \alpha_0\frac{\partial^2\phi_1}{\partial\varsigma^2} = 0, \tag{3.14}$$

$$\frac{\partial\phi_1}{\partial\tau} = \alpha_1^2. \tag{3.15}$$

It should be noted that the system of Equations (3.10), (3.11) is mathematically equivalent to the purely spatial Karman–Guderley equations considered in the theory of steady transonic flows (see [17] Chapter 1, 2). It is interesting to note that it appears now in the context of the description of time-dependent wave-propagation processes.

4. Small-amplitude wave motions near the critical point

In this section we obtain several possible solutions of Equations (3.10), (3.11).

4.1. Steady-state patterns

First consider steady-state solutions of these equations in the following stepwise form

$$\begin{aligned} \alpha_1 &= \alpha\theta(\varsigma) = \alpha\theta\left[\Omega(Y - v_a T)\right], \\ v_1 &= 0 \end{aligned} \tag{4.1}$$

which is valid in both elliptic and hyperbolic regions. In the above equations $\theta(\varsigma)$ is Heaviside's function and a is the amplitude of the step which is of the order of unity and

$$\theta(\varsigma) = \begin{cases} -1, & \varsigma \le 0, \\ 1, & \varsigma > 0. \end{cases} \tag{4.2}$$

This Riemann-type solution describes a frozen symmetrical jump (about α_0) of the particle volume fraction which moves without change of form together with the particulate phase (see Figure 3a). This may occur as a result of instantaneous shifting in the volume fraction at the inlet of the fluidized bed, including α_0. Such a jump transition is shown by the AA' line in Figure 2, where point A corresponds to the initial value of the fraction, *i.e.* α_a. The antisymmetrical jump connects the hyperbolic and elliptic regions.

Equations (3.10), (3.11) have also periodic stationary solutions with any period say, 2π, as shown in Figure 3b. It is a steady-state square-shape pattern. In the next section we shall show that such patterns appear as a result of evolution of a sinusoidal disturbance imposed on a

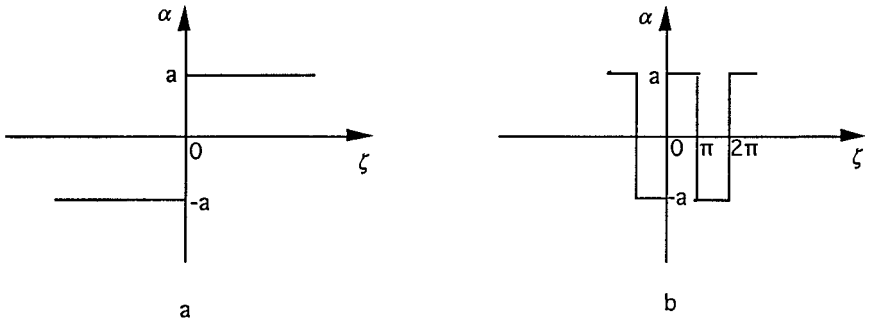

Figure 3. Steady-state configurations of the particle volume fraction: (a) Single symmetrical jump. (b) Periodical square-shape pattern.

uniformly fluidized bed at $\alpha_a = \alpha_0$. Thus, the period of the steady-state pattern is determined by the period of disturbances.

4.2. Self-similar solution

The system of Equations (3.10), (3.11) has a self-similar solution in the hyperbolic region (see [17]). Using the invariance of this system, we can show that it has the following solution

$$\alpha = -\eta^2/2\alpha_0, \quad v = -\eta^3/3\alpha_0, \tag{4.3}$$

where $\eta = \zeta/\tau$. This solution describes an unsteady rarefaction fan stretching in a finite space area.

It should be noted that this self-similar solution does not satisfy the limiting process determined by (2.14), since η is independent of Ω. It therefore does not represent an asymptotic solution of Equations (2.8), (2.9).

4.3. General simple waves

We seek a more general solution of Equations (3.10), (3.11) valid in the hyperbolic region, $\alpha_1 < 0$, assuming that the velocity may be represented as a function of the particle volume fraction, $v_1 = v_1(\alpha_1)$. Then, Equations (3.10), (3.11) can be rewritten as

$$\begin{aligned} &\frac{\partial \alpha_1}{\partial \tau} + \alpha_0 \frac{dv_1}{d\alpha_1}\frac{\partial \alpha_1}{\partial \varsigma} = 0, \\ &\frac{dv_1}{d\alpha_1}\frac{\partial \alpha_1}{\partial \tau} - 2\alpha_1 \frac{\partial \alpha_1}{\partial \varsigma} = 0. \end{aligned} \tag{4.4}$$

The requirement that (4.4) has nontrivial dependence on (ς, τ) results in Equation (3.5). Substituting (3.5) in (4.4) yields the wave equation

$$\frac{\partial \alpha_1}{\partial \tau} \pm \sqrt{-2\alpha_0\alpha_1}\frac{\partial \alpha_1}{\partial \varsigma} = 0, \tag{4.5}$$

where the positive sign yields the back-running wave and the negative sign yields the forward-running wave. Equations (4.5) have implicit solutions

$$\alpha_1 = F(\varsigma \pm \sqrt{-2\alpha_0\alpha_1}\tau), \tag{4.6}$$

where F is nonpositive but otherwise arbitrary function. Both solutions corresponding to positive and negative sign in (4.6) stem from an identical disturbance: $\alpha_1 = F(\varsigma) = F(y)$ at $\tau = 0$, yet the first derivatives of the disturbance with respect to time are different for the back- and the forward-running waves, namely

$$\frac{\partial \alpha_1}{\partial \tau} = \mp\sqrt{-2\alpha_0 F(\varsigma, 0)}F'(\varsigma, 0). \tag{4.7}$$

We now consider in more detail the back-running wave caused by an initially sinusoidal disturbance $\alpha_1 = \sin y = \sin \Omega Y$ in the segment $[\pi, 2\pi]$

$$\alpha_1 = \sin(\varsigma + \sqrt{-2\alpha_0\alpha_1}\tau) = \sin(\Omega Y - \nu_a \Omega T - \sqrt{-2\alpha_0\alpha_1\varepsilon}\Omega T). \tag{4.8}$$

A given value of α_1 moves with the speed $\sqrt{-2\alpha_0\alpha_1}$, so that the sine-wave distorts. A condition $(\partial\varsigma/\partial\alpha_1)_\tau \mid_{\alpha_1=0} = 0$ gives $\tau = 0$. Hence, $\alpha_1(\varsigma)$ becomes instantaneously multivalued at $\varsigma = \pi$. In reality a discontinuity occurs at this point. The location of the discontinuity may be determined by an integral conservation principle resulting from the equal-areas rule (Whitham [18]). Then, for the jump propagation speed, s, we have

$$s = -\frac{2}{3}\sqrt{-2\alpha_0\alpha_{1+}} \tag{4.9}$$

where α_{1+} is the value of the disturbance of the particle volume fraction just behind the jump. Ahead of the jump the particle volume fraction disturbance vanishes. As a result, α_1 turns out to be single-valued everywhere outside the jump.

Let us define a function β as $\beta = \sqrt{-2\alpha_0\alpha_1}$. Then, Equation (4.5) for the back-running wave yields

$$\frac{\partial \beta}{\partial \tau} - \beta\frac{\partial \beta}{\partial \varsigma} = 0. \tag{4.10}$$

Equation (4.10) is the inviscid Burgers' equation with a long-time asymptotic solution described by a sawtooth wave with a linear wave profile (see [18]). In our case α_1 is equal to $-\beta^2$, and the volume-fraction distribution will therefore deviate from the linear one for long times, attaining a parabolic shape. Note that the wave is damped eventually due to energy dissipation.

The simple wave solution obtained above describes wave motions which may occur as a result of a small sinusoidal disturbance in particle density at the inlet of the fluidized bed. This wave can propagate in the fluidized bed, where the particle volume fraction is smaller than (however, close to) the critical value. We have seen that such wave behavior differs qualitatively from that typical for the regions far from the critical point, where evolution of the sinusoidal disturbance is governed by the inviscid Burgers' equation.

4.4. Investigations of small-amplitude periodical wave motions

Propagation of non-unidirectional non-simple waves is now studied. We investigate the instability of the fluidized bed at $\alpha_a = \alpha_0$ with respect to a sinusoidal disturbance. The goal of the investigation is to describe the nonlinear evolution of initially sinusoidal wave trains towards steady-state square-shape patterns (Figure 3b). The initial disturbance is specified by the equations

$$\alpha_1 = \sin\varsigma, \qquad \phi_1 = 0 \qquad 0 \le \varsigma \le 2\pi. \tag{4.11}$$

We solve Equations (3.14), (3.15), which constitute a mathematical problem of mixed type. Specifically, the interval $(0, \pi)$ corresponds to the elliptic region and the interval $(\pi, 2\pi)$ - to the hyperbolic region.

Zeros of the sinusoidal distribution (4.11) correspond to the critical point of the particulate pressure density dependence. In the vicinity of this point the pressure gradient vanishes, provided the particle volume fraction has a spatially anti-symmetric distribution with respect to ς (see (3.11) or (3.15)). The initial disturbance (4.11) satisfies this condition. Therefore, periodic solutions can be constructed subject to the condition of zero pressure gradient on the boundaries $\varsigma = 0, \pi, 2\pi$. This results in the boundary conditions of impermeability

$$\frac{\partial \phi_1}{\partial \varsigma} = 0 \quad \text{at} \quad \varsigma = 0, \pi, 2\pi \tag{4.12}$$

according to which no particles flow through these boundaries. We thus conclude that the spatial average of the particle fraction does not change in time in each of these intervals. Eventually, the sinusoidal wavetrain transforms into a square-shape pattern, representing the steady-state solution. We now determine the height of this pattern resulting from the evolution of the sine-wave. Evaluating the integral mass equation for the initial disturbance (4.11) and the steady-state square-shape configuration (see Figure 3b) we obtain the height as equal to $2/\pi$.

One can observe that the initial sinusoidal disturbance (4.11) and stationary square-shape pattern α_1 (see Figure 3b) are antisymmetrical with respect to ζ. Hence, a continuous solution of Equation (3.11) implies that ν_1 is also antisymmetrical, which clearly contradicts Equation (3.10). However, we look for a discontinuous solution where at the boundaries of the intervals $\varsigma = 0, \pi, 2\pi$ antisymmetric jumps are formed instantaneously which evolve towards their equilibrium height equal to $2/\pi$. In this case, the second term in Equation (3.11) vanishes at these boundaries and no contradiction occurs.

Note that in the interval $0 \leq \varsigma \leq \pi$ the initial-boundary-value problem is of the elliptic type. This is a difficult task. Therefore, we focus further attention on the analysis of evolution of the disturbance in the interval $\pi \leq \varsigma \leq 2\pi$, corresponding to the hyperbolic region. Here we use the physical principles of impermeability and mass conservation in the intervals $0 \leq \varsigma \leq \pi$ and $\pi \leq \varsigma \leq 2\pi$, discussed above, to deduce the eventual steady state in the elliptic region as well. Note that in place of the problem posed by Equations (3.14), (3.15) we can analyze stability of the fluidized bed operation by direct numerical simulations of system (2.15), (2.17) subject to small initial disturbances. This task should apparently meet with similar computational difficulties when simultaneously integrating in the hyperbolic and elliptic regions.

Equations (3.14), (3.15), are solved numerically by a finite-difference method subject to conditions (4.11), (4.12). An explicit scheme is used, where the second derivatives of the potential are approximated by central differences in internal points. In order to approximate the boundary conditions (4.12), two additional points of the spatial grid are introduced just outside the region. The values of the velocity potential at these points are assumed to be equal to those of the closest internal points.

The result of the calculations are presented below, where the number of the internal points of the spatial grid is equal to 99. The relationship between the time step, $\Delta\tau$, and the mesh size of the spatial grid, $\Delta\varsigma$, is as follows: $\Delta\tau = 10^{-3} \cdot \Delta\varsigma^2$.

Figure 4 shows distributions of the particle volume fraction at successive ranges of τ ($\tau = 0,\ 0{\cdot}5,\ 1{\cdot}0$) in the inviscid suspension. We have seen that the stationary plateau is

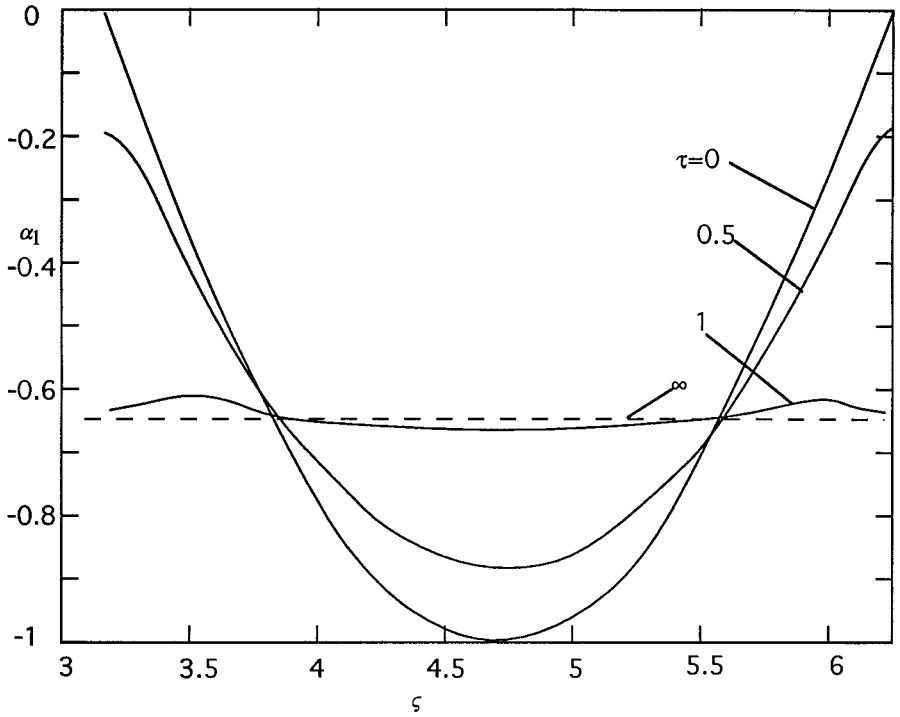

Figure 4. Non-unidirectional periodical wave motions. Interaction of two modes of the initially sine-wave at successive ranges τ.

formed in the region at about time $\tau = 1{\cdot}0$. This transient time may also be expressed as $T = 1/(\Omega\sqrt{\varepsilon})$. Because of the inequality (2.13), this value satisfies the condition (2.18) establishing the validity of the limiting process. The obtained configuration corresponds to the steady-state square-shape pattern with the height $2/\pi$. This pattern develops antisymmetrical jumps at the ends of the interval $(\pi, 2\pi)$. Recalling that such antisymmetrical jumps are steady-state and bearing in mind the mass conservation law, we conclude that the square-shape pattern is to be eventually formed in the interval $(0, \pi)$ also. Thus, the steady-state solution shown in Figure 3b, represents an intermediate asymptotic solution of Equations (2.15), (2.16) valid for large frequencies Ω.

5. Discussions

The result obtained above shows that the uniformly fluidized bed with particle volume fraction equal to its critical value is unstable with respect to oscillations of very high frequencies. This fact is related to the influence of the elliptic region which turns out to be more significant than that of the hyperbolic region. Recall that the purely elliptic disturbance always results in the instability, while the purely hyperbolic disturbance always decays. This represents a new kind of instability unreported in previous studies. In particular, Batchelor [9], who first introduced the barotropic dependence of the particulate pressure on the void fraction in the context of the stability analysis, did not consider stability in the vicinity of the critical point. The influence of the more concentrated elliptic region manifests itself also in the formation of steady-state square-shaped patterns, which occur in our case without any effect of drag

force and gravity. This differs qualitatively from the case analyzed theoretically in [6], where an unstable disturbance of high, but finite, frequency in the hyperbolic region, far from the critical point, is shown to obtain eventually the saw-tooth form with a constant amplitude due to the small effect of gravity and drag force.

Thus, the present study describes theoretically periodical concentration structures occurring as a result of instability in highly concentrated suspensions. This may be important for several processes occurring in concentrated fluidized beds.

Observations of the onset of instabilities of such kind and formation of the steady-state square-shaped patterns represent an important experimental task. Such investigations can, apparently, be performed by means of experimental techniques as described in [14], where concentrational waves and instabilities in uniform bubbly fluidized beds are studied. The latter paper reports experimental results on propagation of small, but finite, amplitude periodic waves, which are in good agreement with classical solutions of the Burgers' equation, describing the formation of the decaying saw-tooth waves. Thus, conditions for experimental observations of the square-shape patterns are readily attainable in experiments.

These studies are also important for further development in investigations of the particulate pressure-volume fraction dependencies in fluidized beds. As we pointed out briefly in the introduction, Zenit et al. [10] measured the collisional particulate pressure in a uniform fluidized bed. It was shown, in particular, that the phenomenological dependence of the particulate pressure on the particle volume fraction as suggested by Batchelor [9], which has a critical point, is in quantitative agreement with experimental data. It should be noted, however, that measurements of particulate pressure are based on the assumption of the existence of this dependence (pressure versus volume-fraction), and show considerable scatter. Observations of square-shape patterns, predicted theoretically in the present work, could provide indirect experimental evidence of the applicability of Batchelor's model.

6. Conclusions

Based on the constitutive equations for gas-solid suspensions, the properties of small-amplitude waves near the point of maximum of the particulate pressure density dependence are investigated in the limit of very high frequencies. The main findings of the investigations are as follows:

– Nonlinear equations describing the wave behavior near the critical point are derived. They represent a system of conservation laws of hyperbolic-elliptic mixed type. The nonlinearity is characterized by the term in the particle momentum equation originating from the particulate pressure gradient and representing a square of the particle volume fraction.

– A steady-state and simple wave solutions are obtained. They describe different wave motions, which may occur as a result of small changes in the particle density at the inlet of the fluidized bed.

– Periodic wave motions in the hyperbolic and elliptic regions near the critical point are studied. Interaction between the two modes of the initial sine-wave of particle concentration (*i.e.* propagating up- and downstream) is examined in the context of a stability analysis. It is shown that the wave transforms into a steady-state square-shape pattern. Such periodic concentration structures may occur in concentrated fluidized beds. Their further theoretical and experimental investigation represents, therefore, an important scientific task.

– The results obtained for small-amplitude waves may be useful for investigating moderate-amplitude concentration-wave propagation in regions containing the critical point of the particulate pressure-density dependence.

Acknowledgements

This work was supported by the Fund for the Promotion of Research at Technion - Israel Institute of Technology. P.V. acknowledges support by TMR Program of European Commission and thanks E.A.Cox for valuable discussions.

References

1. G.J. Kynch, A theory of sedimentation. *Trans. Faraday Soc.* 48, (1952) 166–76.
2. M.J. Lighthill and G.B.Whitham, On kinematic waves. I. Flood movement in long rivers. *Proc. R. Soc. London.* A299 (1955) 281–316.
3. G.H. Ganser and D.A. Drew, Nonlinear stability analysis of a uniformly fluidized bed., *Int. J. Multiphase Flow* 16 (1990) 447–460.
4. A. Kluwick, Weakly nonlinear kinematic waves in suspensions of particles in fluids. *Acta Mecanica* 88 (1991) 205–217.
5. S.E. Harris and D.G. Crighton, Solitons, solitary waves, and voidage disturbance in gas-fluidized beds. *J. Fluid Mech.* 266 (1994) 243–276.
6. A. Kluwick, Small-amplitude finite-rate waves in suspensions of particles in fluids *ZAMM* 63 (1983) 161–171.
7. R. Jackson, The mechanics of fluidized beds. I. The stability of the state of uniform fluidization. *Trans. Inst. Chem. Engrs.* 41 (1963) 13–21.
8. S.K. Gargand and J.W. Pritchett, Dynamics of gas-fluidized beds. *J. Appl. Phys.* 46 (1975) 4493–4500.
9. G.K. Batchelor, A new theory of the instability of a uniform fluidized bed. *J. Fluid Mech.* 193 (1988) 75–110.
10. R. Zenit, M.L. Hunt and C.E. Brennen, Collisional particle pressure measurements in solid-liquid flows. *J. Fluid Mech.* 353 (1997) 261–283.
11. J.B. Fanucci, N. Ness and R. Yen, On the formation of bubbles in gas-particulate fluidized beds. *J. Fluid Mech.* 94 (1979) 353–367.
12. J.H. Lammers and A. Biesheuvel, Concentration waves and the instability of bubbly flows. *J. Fluid Mech.* 328 (1996) 67–93.
13. P. Vainshtein, M. Fichman, M. Shapiro, L. Moldavsky and C. Gutfinger, Fluidized bed in confined volumes. *Int. J. Multiphase Flow* 25 (1999) 1431–1456.
14. A. Goldshtein and M. Shapiro, Mechanics of collisional motion of granular materials Part 1. General hydrodynamic equations. *J. Fluid Mech.* 282 (1995) 75–114.
15. D. Gidaspow, *Multiphase Flow and Fuidization, Continuum and Kinetic theory description.* New York: Academic Press (1994) 521pp.
16. J.F. Richardson and W.N. Zaki, Sedimentation and Fluidization, part I. *Trans. Inst. Chem. Engrs.* 32 (1954) 35–53.
17. J.D. Cole and L.P. Cook, *Transonic Aerodynamics.* Amsterdam: Elsevier (1988) 473pp.
18. G.B. Whitham, 1974 *Linear and Nonlinear Waves.* New York: Wiley (1974) 636pp.